Int. J. Nano Dimens., 6(5): 525-537, 2015, (Special Issue for NCNC, Dec. 2014, IRAN)
DOI: 10.7508/ijnd.2015.05.010

Research Paper

Finite difference method for sixth-order derivatives of differential equations in buckling of nanoplates due to coupled surface energy and non-local elasticity theories

*M. Karimi**, *A. R. Shahidi*

Department of Mechanical Engineering, Isfahan University of Technology, Isfahan 84156-83111, Iran

Received 19 April 2015; revised 18 July 2015; accepted 5 August 2015; available online 01 December 2015

ABSTRACT: In this article, finite difference method (FDM) is used to solve sixth-order derivatives of differential equations in buckling analysis of nanoplates due to coupled surface energy and non-local elasticity theories. The uniform temperature change is used to study thermal effect. The small scale and surface energy effects are added into the governing equations using Eringen's non-local elasticity and Gurtin-Murdoch's theories, respectively. Two different boundary conditions including simply-supported and clamped boundary conditions are investigated. The numerical results are presented to demonstrate the difference between buckling obtained by considering the surface energy effects and that obtained without the consideration of surface properties. The results show that the finite difference method can be used as a powerful method to determine the mechanical behavior of nanoplates. In addition, this method can be used to solve higher-order derivatives of differential equations with different types of boundary condition with little computational effort. Moreover, it is observed that the effects of surface properties tend to increase in thinner and larger nanoplates; and vice versa.

Keywords: *Buckling analysis; Finite difference method; Nanoplate; Non-local elasticity theory; Surface energy theory.*

INTRODUCTION

Nanostructures such as nanoplates, nanobeams and nanotubes have attracted worldwide attention, because of their superior mechanical, thermal and electrical performances. These small-scale nanostructures have wide-ranging applications in many areas such as communications, and in mechanical and biological technologies. In recent years, there has been significant interest in developing micro/nanomechanical and micro/nanoelectromechanical systems (MEMS/NEMS), such as capacitive sensor, switches, actuators, and so on. These devices can be contributed to novel technological developments in many fields leading to industrial revolution [1, 2]. The continuum mechanics approaches are widely preferred due to their simplicity. The main feature of structures is their high surface-to-volume ratio, which makes elastic response of their surface layers to be different from macroscale structures. That is why Gurtin and Murdoch [3, 4] developed a theoretical framework based on continuum mechanics concepts that included the effects of surface and interfacial energies. In their approach, the surface was modeled as a mathematical layer of zero thickness perfectly bonded to an underlying bulk substance. The surface (interface) had its own properties, which were different from those of the bulk material. These properties, such as surface energies, affect on physical, mechanical, and electrical properties as well as mechanical response of the nanostructure and can cause interesting behaviors. For example, Assadi [5] and Assadi et al. [6] investigated force and free vibration of nanoplates considering surface energy effects. Moreover, Assadi and Farshi [7, 8] studied surface energy effects on the vibration and buckling of circular nanoplate. They showed that surface energy effects could have significant effects on the nanostructures. Moreover, increasing in the thickness causes reduction of the surface energy effects. Ansari and Sahmani [9] analyzed bending and

*Corresponding Author: Morteza Karimi
Email: *morteza.karimi@me.iut.ac.ir*
Tel.: (+98) 311391-5237
Fax: (+98) 311391-5216

buckling of nanobeams by considering surface stress effects and normal stresses, using different beam theories. They showed that the difference between the behaviors of nanobeams predicted by with and without surface effects would depend on the magnitudes of the surface elastic constants. In these works [5-9], because of using classical solutions, e.g., Navier's method as used for simply-supported boundary conditions, the above-mentioned researchers were not able to study other boundary conditions.

Challamel and Elishakoff [10] analyzed buckling of nanobeams, incorporating the surface stress effects into the Euler–Bernoulli and Timoshenko beam theories. They explained that the surface elasticity effects may soften a nanostructure for some specific boundary condition. Recently, Karimi *et al.* [11] studied size-dependent free vibration analysis of rectangular nanoplates with the consideration of surface energy effects using finite difference method (FDM). They reported that the effects of surface properties tend to diminish in thicker nanoplates, and vice versa. Recently, Ansari *et al.* [12] investigated surface energies effects on the buckling, and maximum deflection of nanoplates using first order shear deformation plate theory and generalized differential quadrature method (GDQM). Moreover, they [13] analyzed forced vibration of Timoshenko nanobeams based on the surface stress elasticity theory using GDQM. They reported that the significance of surface energy effects on the response of nanoplate would rely on its size, type of edge supports, and the selected surface constants. On the other hand, Mouloodi *et al.* [14, 15] analyzed the surface energy effects on the bending and vibration of multicrystalline nanoplate. Furthermore, Wang and Wang [16] studied the surface energy effects on the bending and vibration of Mindlin nanoplates. In these works [14-16], the finite element method (FEM) was utlized to solve governing equations based on classical beam and plate theories. They explained that depending on the boundary conditions, the deflections and frequencies of nanoplates had a dramatic dependence on the surface energy effects. In these works [5-16], the effect of non-local parameter was not considered into governing equations. On the other hand, the order derivatives of differential equations in buckling and vibration were less or equal fourth-order.

In nanoscale, the small scale effects cannot be ignored. That is why, some researchers investigated the effects of surface energy effects on the buckling and vibration considering nonlocal elasticity theory. For example, Wang and Wang [17, 18] studied buckling and vibration of rectangular nanoplates including both surface energy and non-local elasticity using *Navier's method*. They explained that by increasing the value of non-local parameter, the surface energy effects could decrease. Farajpour *et al.* [19, 20] analyzed the surface energy and non-local effects on the axisymmetric buckling and vibration of circular graphene sheets in thermal environment using DQM. They [19, 20] studied only clamped boundary condition. They showed that the size effects would decrease with an increase in the value of surface residual stresses. In these works [17-20], the small scale effects were only considered for the bulk of nanoplates.

On the other hand, some researchers investigated surface energy effects on the buckling and vibration of nanobeams and nanoplates including non-local parameter into both nanoplate bulk and surface. For examples, Mahmoud *et al.* [21] studied static analysis of nanobeams including surface energy effects into governing equations using non-local finite element method. Moreover, Eltaher *et al.* [22] combined effects of non-local and surface energy on the vibration of nanobeams. They used an efficiently finite element model to descretize nanobeam domain and solve the equation of motion numerically. They showed that the surface properties have significant effects when the thickness of beam structure approaches to its intrinsic length. Recently, Karimi *et al.* [23] Combined surface energy effects and non-local two variable refined plate theories on the buckling and vibration of rectangular nanoplates using DQM. They explained that the non-local effects on the shear buckling and vibration are more important than that of biaxial buckling and vibration. Shokrani *et al.* [24] investigated buckling analysis of double-orthotropic nanoplates embedded in elastic media based on non-local two-variable refined plate theory using GDQM without considering surface energy effects. They showed that the effects of non-local parameter for shear buckling are more noticeable than that of biaxial buckling.

It should be noted that, with considering non-local parameter for only nanoplate bulk [17-20], in the final equations displacement nanoplates sixth-order derivatives appear. In this case, for solving equations with numerical methods we need three boundary conditions for any edge of nanoplates. But in the work [19, 20] two boundary conditions were considered. In this case, the answer of equations might be wrong. But when the non-local effects considered for both bulk and surface [21-23], in the final equations displacement nanoplates fourth-order derivatives appear. In this case, for solving equations with numerical methods we need two boundary conditions for any edge of nanoplates. In this case, the numerical methods for solving equations with various boundary conditions could be done easily. On the other hand, the answer of equations for two cases, consideration of non-local parameter for only bulk and for both bulk and surface of nanoplates are different.

In recent years some researchers studied influence of magnetic field on the nanofluids. For example, Sheikholeslami and Rashidi [25] investigated effect of space dependent magnetic field on free convection of Fe3O4-water nanofluid. They indicated that enhancement in heat transfer decrease with increasing of Rayleigh number, while for two other active parameters different behavior was observed. Moreover, Sheikholeslami and Domiri Ganji [26] analyzed nanofluid flow and heat transfer between parallel plates considering Brownian motion using DTM. They reported that skin friction coefficient would increase with increasing of the squeeze number and Hartmann number but it was decreased with increasing of nanofluid volume fraction. Recently, Sheikholeslami *et al.* [27] studied lattice Boltzmann method for simulation of magnetic field effect on hydrothermal behavior of nanofluid in a cubic cavity. They showed that enhancement in heat transfer has direct relationship with Hartmann number, while it had inverse relationship with Rayleigh number. In addition, they [28] investigated magnetic field effects on natural convection around a horizontal circular cylinder inside a square enclosure filled with nanofluid. They reveal that the average Nusselt number was an increasing function of nanoparticle volume fraction as well as the Rayleigh number, while it was a decreasing function of the Hartmann number. Soleimani *et al.* [29] studied natural convection heat transfer in a nanofluid filled semi-annulus enclosure. They reported that there was an optimum angle of turn in which the average Nusselt number is maximum for each Rayleigh number.

The main objective of this article is to numerically investigation. In the present work, FDM is used to solve sixth-order derivatives of differential equations in buckling analysis of nanoplates due to coupled surface energy and non-local elasticity theories. The uniform temperature change is used to study thermal effect. In this article, small-scale and surface effects are introduced using the Eringen's non-local elasticity and Gurtin-Murdoch's theory, respectively. Two different boundary conditions including simply-supported and clamped boundary conditions are investigated. First, the governing differential equation is introduced according to the literature, and then this equation is solved using the FDM to obtain the buckling for several combinations of boundary conditions. To verify the accuracy of the results obtained by the FDM, these results are compared with the results of the analytical approach.

EXPERIMENTAL

Coupling surface energy and non-local elasticity theories

By using non-local elasticity theory [30] and disregarding body forces, the stress equilibrium equation for a linear homogeneous non-local elastic body can be written as:

$$\pm_{ij}^{nl} = \int_{¸} (|x - x'|, ¥) C_{ijkl} £_{kl}(x') dV(x') \qquad \forall x \in V \tag{1}$$

Here, $\pm_{ij}^{nl}$, $£_{ij}$ and C_{ijkl} are the stress, strain and fourth-order elasticity tensor, respectively. ¸($|x$-$x'|$, ¥) is regarded as a non-local modulus, %x-x'% represents a Euclidean distance and ¥ is a material constant ¥=$e_0\, a_0$ /l) depending on the internal characteristics length, a and external characteristic length, l. Parameter a is a lattice parameter, granular size, or the distance between C–C bonds. Parameter e_0 is estimated such that relations of non-local elasticity model could provide satisfactory atomic dispersion curves of plane waves by using approximations from atomic lattice dynamics. Since a constitutive law of integral form is difficult to implement, a simplified differential form of Eq. (1) is used as the basis:

$$(1 - g^2 \nabla^2) \pm_{ij}^{nl} = C_{ijkl} £_{kl} \tag{2}$$

In the above equation, $\nabla^2 = (\partial^2/\partial x^2) + (\partial^2/\partial y^2)$ is the Laplacian. $g^2 = (e_0\, a_0)^2$ is the non-local parameter. The force and moment resultants of the non-local elasticity can be defined as [17, 18]:

$$\begin{aligned} (N_{xx}, N_{yy}, N_{xy}) &= \int_{-h/2}^{h/2} (\sigma_{xx}^{nl}, \sigma_{yy}^{nl}, \sigma_{xy}^{nl})\, dz \\ (M_{xx}, M_{yy}, M_{xy}) &= \int_{-h/2}^{h/2} (\sigma_{xx}^{nl}, \sigma_{yy}^{nl}, \sigma_{xy}^{nl})\, z\, dz \end{aligned} \tag{3}$$

Here, h denotes the thickness of the nanoplates. $\sigma_{xx}{}^{nl}$, $\sigma_{yy}{}^{nl}$, and $\sigma_{xy}{}^{nl}$ are the non-local stresses, where the superscript *nl* denotes “non-local”. The displacement components in the x and y directions are obtained from the Kirchhoff’s plate model, as follows [11, 17, 18]:

$$v=-z\frac{\partial w}{\partial y}\ u=-z\frac{\partial w}{\partial x}, \tag{4}$$

The resulting strain components in the Cartesian coordinates can be derived by using the relations of Eq. (3), which are always considered to be the same for both nanoplates bulk and surface [11, 17, 18]:

$$\varepsilon_{yy}=-z\frac{\partial^2 w}{\partial y^2},\ \gamma_{xy}=-2z\frac{\partial^2 w}{\partial x\partial y}\ \varepsilon_{xx}=-z\frac{\partial^2 w}{\partial x^2} \tag{5}$$

As was discussed in the previous section, the external layers of all the elastic solids have additional material properties. Based on the Gurtin-Murdoch theory of elastic solid surfaces [3], the stress-strain relations of surface nanoplates are expressed by [11, 17, 18, 23]:

$$\begin{aligned}&\sigma^{s}_{\alpha\beta}=\tau^{s}\delta_{\alpha\beta}+(\mu^{s}-\tau^{s})(u_{\alpha,\beta}+u_{\alpha,\beta})+\\&(\tau^{s}+\lambda^{s})u_{\gamma,\gamma}\delta_{\alpha\beta}+\tau^{s}u_{\alpha,\beta}\qquad (z=\pm\frac{h}{2})\\&\sigma^{s}_{\alpha\beta}=\tau^{s}\frac{\partial w}{\partial x_{\alpha}}\qquad (z=\pm\frac{h}{2})\end{aligned} \tag{6}$$

where α=β=¥=1,2. In Eq. (6), λs and μs are the surface Lame constants. Substituting the strain components from Eq. (5) into Eq. (6) yields additional surface stress components in terms of transverse displacement (w), as follows[11, 17, 18, 23]:

$$\begin{aligned}\sigma^{s\pm}_{xx}&=\tau^{s}+(2\mu^{s}+\lambda^{s})u_{,x}+(\tau^{s}+\lambda^{s})v_{,y}\\&=\tau\mp\frac{h}{2}\left\{(2\mu^{s}+\lambda^{s})\frac{\partial^2 w}{\partial x^2}+(\tau^{s}+\lambda^{s})\frac{\partial^2 w}{\partial y^2}\right\}\\\sigma^{s\pm}_{yy}&=\tau^{s}+(2\mu^{s}+\lambda^{s})v_{,y}+(\tau^{s}+\lambda^{s})u_{,x}\\&=\tau\mp\frac{h}{2}\left\{(2\mu^{s}+\lambda^{s})\frac{\partial^2 w}{\partial y^2}+(\tau^{s}+\lambda^{s})\frac{\partial^2 w}{\partial x^2}\right\}\end{aligned} \tag{7}$$

$$\begin{aligned}\sigma^{s\pm}_{xy}&=\mu^{s}(u_{,y}+v_{,x})-\tau^{s}v_{,x}\\&=\mp\frac{h}{2}(2\mu^{s}-\tau^{s})\frac{\partial^2 w}{\partial x\partial y}\\\sigma^{s}_{xz}&=\tau^{s}\frac{\partial w}{\partial x}\ ,\quad \sigma^{s}_{yz}=\tau^{s}\frac{\partial w}{\partial y}\end{aligned}$$

In the above relations, superscripts + and represent the upper and lower surfaces of nanoplate, respectively. The resultant stresses are obtained by the following integral equations [11, 17, 18, 23]:

$$\begin{aligned}M_{xx}&=(\sigma^{s+}_{xx}-\sigma^{s-}_{xx})\frac{h}{2}+\int_{-h/2}^{h/2}\sigma^{nl}_{xx}z\,dz\\M_{yy}&=(\sigma^{s+}_{yy}-\sigma^{s-}_{yy})\frac{h}{2}+\int_{-h/2}^{h/2}\sigma^{nl}_{yy}z\,dz\\M_{xy}&=(\sigma^{s+}_{xy}-\sigma^{s-}_{xy})\frac{h}{2}+\int_{-h/2}^{h/2}\sigma^{nl}_{xy}z\,dz\end{aligned} \tag{8}$$

Using the principle of virtual work, the governing equations of nanoplates subjected to thermal effect can be obtained as [11, 17, 18]:

$$\begin{aligned}&N_{xx,x}+N_{xy,y}=0\\&N_{yy,y}+N_{xy,x}=0\\&M_{xx,xx}+M_{yy,yy}+2M_{xy,xy}+(\sigma^{s+}_{\alpha z}+\sigma^{s-}_{\alpha z})_{,\alpha}\\&+(N_{xx}+N^{T}_{xx})w_{,xx}+(N_{yy}+N^{T}_{yy})w_{,yy}\\&+(N_{xy}+N^{T}_{xy})w_{,xy}=0\end{aligned} \tag{9}$$

where α=x, y. the non-local stress-strain relations of bulk material subjected to thermal effect are written as [17-20, 23]:

$$\begin{Bmatrix}\pm^{nl}_{xx}\\\pm^{nl}_{yy}\\\pm^{nl}_{xy}\end{Bmatrix}-g^{2}\nabla^{2}\begin{Bmatrix}\pm^{nl}_{xx}\\\pm^{nl}_{yy}\\\pm^{nl}_{xy}\end{Bmatrix}=\begin{bmatrix}E/(1-¬^{2}) & ¬E/(1-¬^{2}) & 0\\¬E/(1-¬^{2}) & E/(1-¬^{2}) & 0\\0 & 0 & G\end{bmatrix}\begin{Bmatrix}£_{xx}\\£_{yy}\\¥_{xy}\end{Bmatrix}-\begin{Bmatrix}E\sim\Delta T/(1-¬)\\E\sim\Delta T/(1-¬)\\0\end{Bmatrix} \tag{10}$$

where E, v, and G denote the elastic modulus, Poisson's ratio, and shear modulus of the nanoplate, respectively. where α and ΔT represent the thermal expansion coefficient and temperature change, respectively. Using Eqs. (3), (5) and (10), we obtain [17-20, 23]:

$$\begin{Bmatrix} M_{xx} \\ M_{yy} \\ M_{xy} \end{Bmatrix} - g^2\nabla^2 \begin{Bmatrix} M_{xx} \\ M_{yy} \\ M_{xy} \end{Bmatrix} = -D\begin{bmatrix} 1 & \nu & 0 \\ \nu & 1 & 0 \\ 0 & 0 & \frac{1-\nu}{2} \end{bmatrix} \begin{Bmatrix} \frac{\partial^2 w}{\partial x^2} \\ \frac{\partial^2 w}{\partial y^2} \\ 2\frac{\partial^2 w}{\partial x \partial y} \end{Bmatrix} \qquad (11)$$

where $D=Eh^3/12(1\text{-}v^2)$ is the classical flexural rigidity of the nanoplate without the consideration of surface effects. Thermal effect can cause bending and buckling in the nanoplates. According to the theory of thermal elasticity, the thermal force can be expressed as [17-20]:

$$N_{xx}^T = N_{yy}^T = -\frac{Eh\alpha}{(1-\nu)}\Delta T$$
$$N_{xy}^T = 0 \qquad (12)$$

Using Eqs. (7), (9), (11) and (12) and assuming the same properties for the upper and lower surfaces, we can obtain the following governing equation:

$$\begin{aligned} &\left((D+\frac{h^2E^s}{2})(\frac{\partial^4 w}{\partial x^4}+2\frac{\partial^4 w}{\partial x^2\partial y^2}+\frac{\partial^4 w}{\partial y^4}) \right) - \frac{g^2h^2E^s}{2} \\ &\left((\frac{\partial^6 w}{\partial x^6}+3\frac{\partial^6 w}{\partial x^4\partial y^2}+3\frac{\partial^6 w}{\partial x^2\partial y^4}+\frac{\partial^6 w}{\partial y^6}) \right) \\ &-\left((2\tau^s-\frac{Eh\alpha}{(1-\nu)}\Delta T)(\frac{\partial^2 w}{\partial x^2}+\frac{\partial^2 w}{\partial y^2}) \right) + g^2 \\ &\left((2\tau^s-\frac{Eh\alpha}{(1-\nu)}\Delta T)(\frac{\partial^4 w}{\partial x^4}+2\frac{\partial^4 w}{\partial x^2\partial y^2}+\frac{\partial^4 w}{\partial y^4}) \right) \\ &-\left(N_{xx}\frac{\partial^2 w}{\partial x^2}+N_{xy}\frac{\partial^2 w}{\partial x\partial y}+N_{yy}\frac{\partial^2 w}{\partial y^2} \right) + g^2 \\ &\left((\frac{\partial^2 w}{\partial x^2}+\frac{\partial^2 w}{\partial y^2})(N_{xx}\frac{\partial^2 w}{\partial x^2}+N_{xy}\frac{\partial^2 w}{\partial x\partial y}+N_{yy}\frac{\partial^2 w}{\partial y^2}) \right) = 0 \end{aligned} \qquad (13)$$

where $E^s=2\mu^s+\lambda^s$. For simplicity, the following nomenclature is used for uniform biaxial compression ratios (see Fig.1)

$$N_{xx} = N \; , \; N_{yy} = N \; , \; N_{xy} = 0 \qquad (14)$$

The finite difference method is a powerful method for solving differential equations. Recently, Karamooz Ravari *et al.* [31, 32] studied non-local effect on the buckling of rectangular, circular, and annular nanoplates using finite difference method. Moreover, Karimi *et al.* [11] investigated size-dependent free vibration analysis of rectangular nanoplates with the consideration of surface energy effects but without considering non-local effect using finite difference method. The finite difference method replaces the nanoplate differential equation and the expressions defining the boundary conditions with equivalent differences equations. The solution of the bending problem thus reduces to the simultaneous solution of a set of algebraic equations written for every nodal point within the nanoplate. Fig. 2 shows a rectangular nanoplate and the grid points which will be used in the finite difference method. By using this method, Eq. (15) can be used to estimate the derivative of the transverse displacement, w, for the i,j-th point as a function of its neighboring points.

$$\frac{dw}{dx} = \frac{1}{2r_x}(w_{(i+1,j)} - w_{(i-1,j)})$$

$$\frac{dw}{dy} = \frac{1}{2r_y}(w_{(i,j+1)} - w_{(i,j-1)})$$

$$\frac{d^2w}{dx^2} = \frac{1}{r_x^2}(w_{(i+1,j)} - 2\,w_{(i,j)} + w_{(i-1,j)})$$

$$\frac{d^2w}{dy^2} = \frac{1}{r_y^2}(w_{(i,j+1)} - 2\,w_{(i,j)} + w_{(i,j-1)}) \qquad (15)$$

$$\frac{d^4w}{dx^4} = \frac{1}{r_x^4}(w_{(i+2,j)} - 4\,w_{(i+1,j)} + 6\,w_{(i,j)} - 4\,w_{(i-1,j)} + w_{(i-2,j)})$$

$$\frac{d^4w}{dy^4} = \frac{1}{r_y^4}(w_{(i,j+2)} - 4\,w_{(i,j+1)} + 6\,w_{(i,j)} - 4\,w_{(i,j-1)} + w_{(i,j-2)})$$

$$\frac{d^4w}{dx^2dy^2} = \frac{1}{r_x^2r_y^2}\begin{pmatrix} w_{(i+1,j+1)} + w_{(i-1,j+1)} \\ + w_{(i-1,j-1)} + w_{(i+1,j-1)} + 4\,w_{(i,j)} \\ -2(w_{(i+1,j)} + w_{(i,j+1)} + w_{(i-1,j)} + w_{(i,j-1)}) \end{pmatrix}$$

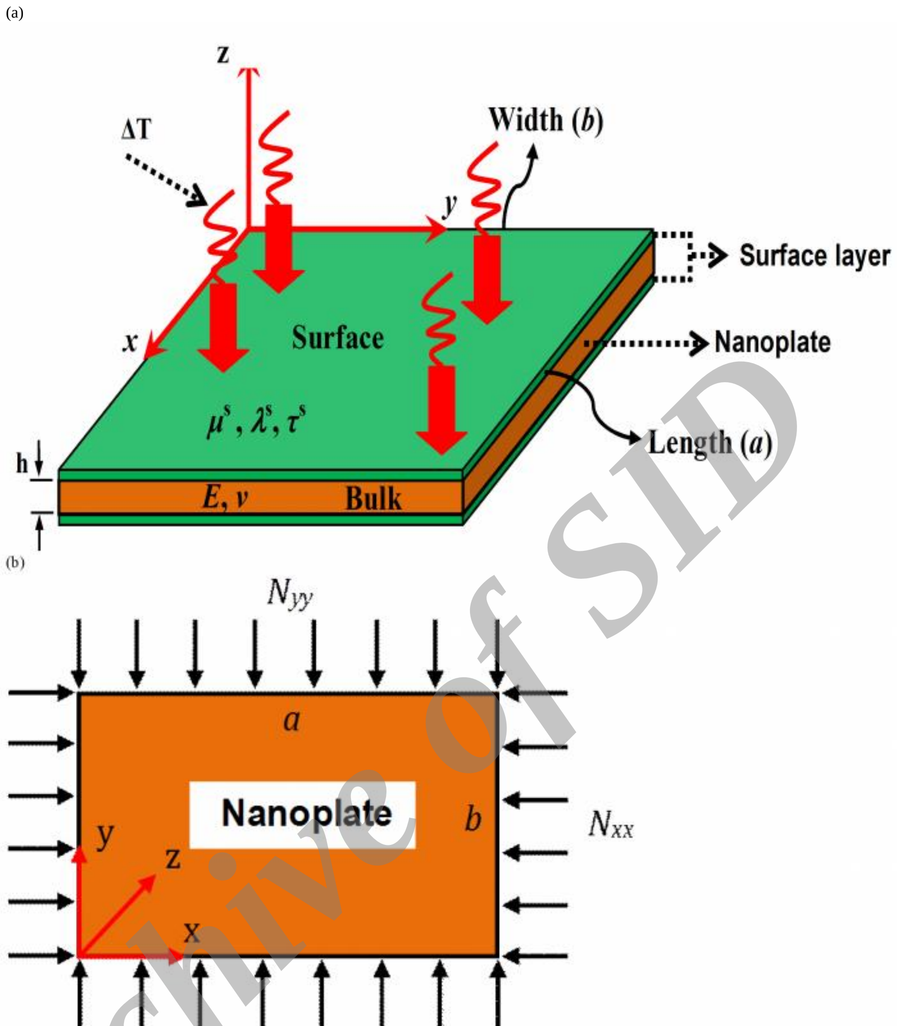

Fig. 1 (a): The geometry of rectangular nanoplate with surface layers and thermal loading, (b) biaxial loading

$$\frac{d^6w}{dx^6}=\frac{1}{r_x^6}\begin{pmatrix} w_{(i-3,j)}-6w_{(i-2,j)}+15w_{(i-1,j)} \\ -20w_{(i,j)}+15w_{(i-1,j)}-6w_{(i-2,j)}+w_{(i-3,j)} \end{pmatrix}$$

$$\frac{d^6w}{dy^6}=\frac{1}{r_y^6}\begin{pmatrix} w_{(i,j-3)}-6w_{(i,j-2)}+15w_{(i,j-1)} \\ -20w_{(i,j)}+15w_{(i,j-1)}-6w_{(i,j-2)}+w_{(i,j-3)} \end{pmatrix}$$

$$\frac{d^6w}{dx^4dy^2}=\frac{1}{r_x^4r_y^2}\begin{pmatrix} w_{(i-2,j+1)}-2w_{(i-2,j)}+w_{(i-2,j-1)} \\ -4w_{(i-1,j+1)}+8w_{(i-1,j)}-4w_{(i-1,j-1)} \\ +6w_{(i,j+1)}-12w_{(i,j)}+6w_{(i,j-1)} \\ -4w_{(i+1,j+1)}+8w_{(i+1,j)}-4w_{(i+1,j-1)} \\ +w_{(i+2,j+1)}-2w_{(i+2,j)}+w_{(i+2,j-1)} \end{pmatrix}$$

$$\frac{d^6w}{dx^2dy^4}=\frac{1}{r_x^2r_y^4}\begin{pmatrix} w_{(i+1,j-2)}-2w_{(i,j-2)}+w_{(i-1,j-2)} \\ -4w_{(i+1,j-1)}+8w_{(i,j-1)}-4w_{(i-1,j-1)} \\ +6w_{(i+1,j)}-12w_{(i,j)}+6w_{(i-1,j)} \\ -4w_{(i+1,j+1)}+8w_{(i,j+1)}-4w_{(i-1,j+1)} \\ +w_{(i+1,j+2)}-2w_{(i,j+2)}+w_{(i-1,j+2)} \end{pmatrix} \tag{15}$$

Here r_x and r_y are the distance between two grid points in the x and y directions, respectively. Substituting Eq. (15) into Eq. (13) and developing a computer code in MATLAB the governing equation are solved.

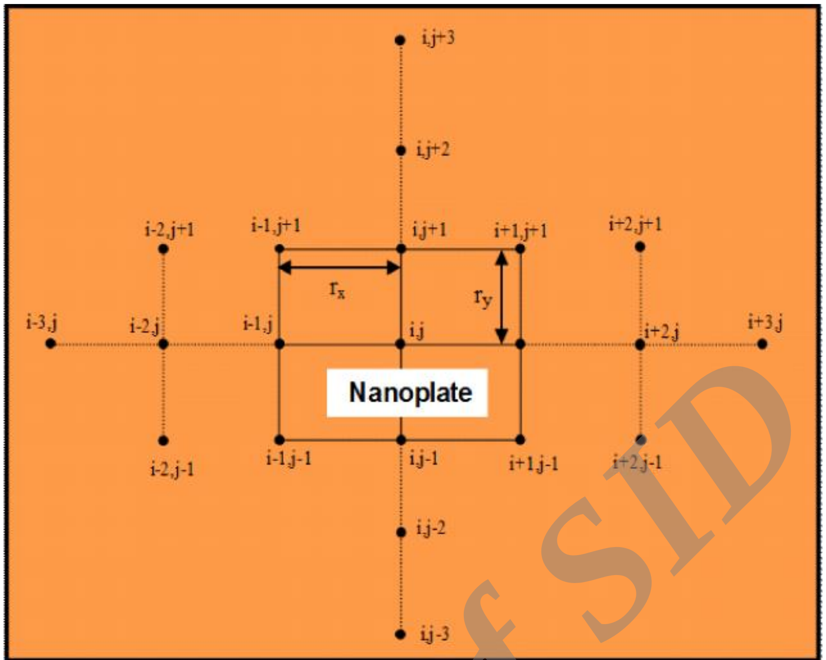

Fig. 2: The rectangular nanoplate and finite difference grid points

$$
\begin{aligned}
&\left(D+\frac{h^2E^s}{2}+2\,2^{s}g^2-\frac{Eh\sim}{(1-\neg)}\Delta T\, g^2\right)\\
&\Bigg\{\frac{1}{r_x^4}\big(w_{(i+2,j)}-4\,w_{(i+1,j)}+6\,w_{(i,j)}\\
&-4\,w_{(i-1,j)}+w_{(i-2,j)}\big)+\frac{1}{r_y^4}\\
&\big(w_{(i,j+2)}-4\,w_{(i,j+1)}+6\,w_{(i,j)}-4\,w_{(i,j-1)}+w_{(i,j-2)}\big)\\
&+\frac{2}{r_x^2r_y^2}\big(w_{(i+1,j+1)}+w_{(i-1,j+1)}+w_{(i-1,j-1)}+w_{(i+1,j-1)}+4\,w_{(i,j)}\big)\\
&-\frac{4}{r_x^2r_y^2}\big(w_{(i+1,j)}+w_{(i,j+1)}+w_{(i-1,j)}+w_{(i,j-1)}\big)\Bigg\}\\
&+\left(-2\,2^{s}+\frac{Eh\sim}{(1-\neg)}\Delta T\right)\Bigg\{\frac{1}{r_x^2}\big(w_{(i+1,j)}-2\,w_{(i,j)}+w_{(i-1,j)}\big)\\
&+\frac{1}{r_y^2}\big(w_{(i,j+1)}-2\,w_{(i,j)}+w_{(i,j-1)}\big)\Bigg\}\\
&-\frac{g^2h^2E^s}{2}\Bigg\{\frac{1}{r_x^6}\left(\begin{array}{l}w_{(i-3,j)}-6\,w_{(i-2,j)}+15\,w_{(i-1,j)}\\-20\,w_{(i,j)}+15\,w_{(i-1,j)}-6\,w_{(i-2,j)}+w_{(i-3,j)}\end{array}\right)\\
&+\frac{1}{r_y^6}\left(\begin{array}{l}w_{(i,j-3)}-6\,w_{(i,j-2)}+15\,w_{(i,j-1)}-20\,w_{(i,j)}\\+15\,w_{(i,j-1)}-6\,w_{(i,j-2)}+w_{(i,j-3)}\end{array}\right)\\
&+\frac{3}{r_x^4r_y^2}\left(\begin{array}{l}w_{(i-2,j+1)}-2\,w_{(i-2,j)}+w_{(i-2,j-1)}\\-4\,w_{(i-1,j+1)}+8\,w_{(i-1,j)}-4w_{(i-1,j-1)}\\+6w_{(i,j+1)}-12\,w_{(i,j)}+6w_{(i,j-1)}\\-4\,w_{(i+1,j+1)}+8\,w_{(i+1,j)}-4w_{(i+1,j-1)}\\+w_{(i+2,j+1)}-2\,w_{(i+2,j)}+w_{(i+2,j-1)}\end{array}\right)\\
&+\frac{3}{r_x^2r_y^4}\left(\begin{array}{l}w_{(i+1,j-2)}-2\,w_{(i,j-2)}+w_{(i-1,j-2)}\\-4\,w_{(i+1,j-1)}+8\,w_{(i,j-1)}-4w_{(i-1,j-1)}\\+6w_{(i+1,j)}-12\,w_{(i,j)}+6w_{(i-1,j)}\\-4\,w_{(i+1,j+1)}+8\,w_{(i,j+1)}-4w_{(i-1,j+1)}\\+w_{(i+1,j+2)}-2\,w_{(i,j+2)}+w_{(i-1,j+2)}\end{array}\right)\Bigg\}\\
&+N_{xx}\Bigg\{\frac{1}{r_x^2}\big(w_{(i+1,j)}-2\,w_{(i,j)}+w_{(i-1,j)}\big)\\
&+\frac{1}{r_x^2r_y^2}\big(w_{(i+1,j+1)}+w_{(i-1,j+1)}+w_{(i-1,j-1)}
\end{aligned}
\qquad (16)
$$

$$+w_{(i+1,j-1)}+4w_{(i,j)}\Big)-\frac{2}{r_x^2 r_y^2}\begin{pmatrix} w_{(i+1,j)}+w_{(i,j+1)} \\ +\ w_{(i-1,j)}+w_{(i,j-1)} \end{pmatrix}\Bigg\}$$

$$+N_{yy}\left\{\begin{array}{l} \frac{1}{r_y^2}\left(w_{(i,j+1)}-2w_{(i,j)}+w_{(i,j-1)}\right) \\ +\frac{1}{r_x^2 r_y^2}\Big(w_{(i+1,j+1)}+w_{(i-1,j+1)}+w_{(i-1,j-1)} \end{array}\right. \tag{16}$$

$$+w_{(i+1,j-1)}+4w_{(i,j)}\Big)-\frac{2}{r_x^2 r_y^2}\begin{pmatrix} w_{(i+1,j)}+w_{(i,j+1)} \\ +\ w_{(i-1,j)}+w_{(i,j-1)} \end{pmatrix}\Bigg\}=0$$

Boundary conditions

In this paper, simply-supported and clamped boundary conditions are surveyed at all plate edges. The boundary conditions are written as:

Simply-supported boundary conditions

The simply-supported boundary conditions at all edges of nanoplate can be written as:

$$\frac{\partial^2 w}{\partial x^2}=0$$
$$\frac{\partial^2 w}{\partial y^2}=0 \tag{17}$$
$$w=0$$

These conditions lead to the following expressions:

$$\begin{aligned} &w_{(i,j)}=-w_{(i,j+2)},\quad w_{(i,j)}=-w_{(i,j-2)},\\ &w_{(i,j+3)}=-w_{(i,j-1)},\quad w_{(i,j-3)}=-w_{(i,j+1)}\\ &w_{(i,j)}=-w_{(i-2,j)},\quad w_{(i,j)}=-w_{(i+2,j)},\\ &w_{(i-3,j)}=-w_{(i+1,j)},\quad w_{(i+3,j)}=-w_{(i-1,j)}\\ &w_{(i,j\pm1)}=w_{(i+1,j\pm1)}=w_{(i-1,j\pm1)}=w_{(i\pm1,j)}=0 \end{aligned} \tag{18}$$

Clamped boundary conditions

The clamped boundary conditions could be expressed as follows:

$$\frac{\partial w}{\partial x}=0$$
$$\frac{\partial w}{\partial y}=0 \tag{19}$$
$$w=0$$

These conditions lead to the following expressions:

$$\begin{aligned} &w_{(i,j)}=w_{(i,j+2)},\quad w_{(i,j)}=w_{(i,j-2)},\\ &w_{(i,j+3)}=w_{(i,j-1)},\quad w_{(i,j-3)}=w_{(i,j+1)}\\ &w_{(i,j)}=w_{(i-2,j)},\quad w_{(i,j)}=w_{(i+2,j)},\\ &w_{(i-3,j)}=w_{(i+1,j)},\quad w_{(i+3,j)}=w_{(i-1,j)}\\ &w_{(i,j\pm1)}=w_{(i+1,j\pm1)}=w_{(i-1,j\pm1)}=w_{(i\pm1,j)}=0 \end{aligned} \tag{20}$$

RESULTS AND DISCUSSION

In this section, it is attempted to demonstrate the surface, thermal, and non-local effects (small scale effects) on the buckling of rectangular nanoplates. The critical buckling load ratio is (CBLR) defined in the following from:

$$CBLR=\frac{\textit{buckling load with both non-local and surface energy theories}}{\textit{buckling load without both non-local and surface energy theories}} \tag{21}$$

Table 1 shows the numerical results for buckling ratio of silver nanoplates with simply-supported boundary conditions versus mode number, *m*. The material properties of silver nanoplates in all examples are taken as E=76 *GPa* and ν=0.3. Surface elastic modulus, surface residual stress are E^s=1.22 *N/m*, τ^s=0.89 *N/m*, respectively. From Table 1, good agreements can be observed between the FDM results and the results in [17]. The results in [17] are based on an exact analytical solution. Thus, the obtained results can be trusted.

Finite difference method results are sensitive to lower grid points, a convergence test is performed to determine the minimum number of grid points required to obtain stable and accurate results for Eq. (16). In Fig. 3, non-dimensional buckling load ($N a^2/D$) is plotted versus the number of grid points for various non-local parameters. According to Fig. 3, the present solution is converging. From this figure, it is clearly seen that 12 number of grid points (N=M=12) are sufficient to obtain the accurate solutions for the buckling analyses. *N* and *M* are the number of grid points in the *x* and *y* directions, respectively.

Fig. 4(a and b) show the effects of non-local parameters on the critical buckling load ratio (CBLR) of nanoplates with simply-supported (SSSS) and

Table 1: CBLR for silver nanoplates with simply-supported boundary conditions (h=5 nm, E^s =1.22 *N/m*, τ^s=0.89 *N/m*, ΔT =0)

		a=10 *nm*				a=20 *nm*			
g^2 nm^2		m=1	2	3	4	m=1	2	3	4
0	FDM	1.028	1.022	1.020	1.019	1.059	1.034	1.026	1.023
	[17]	1.028	1.022	1.020	1.019	1.059	1.034	1.026	1.023
1	FDM	0.860	0.690	0.520	0.391	1.012	0.923	0.828	0.729
	[17]	0.863	0.691	0.523	0.392	1.012	0.924	0.828	0.727
2	FDM	0.744	0.521	0.350	0.242	0.968	0.834	0.695	0.568
	[17]	0.745	0.525	0.356	0.248	0.969	0.836	0.695	0.566

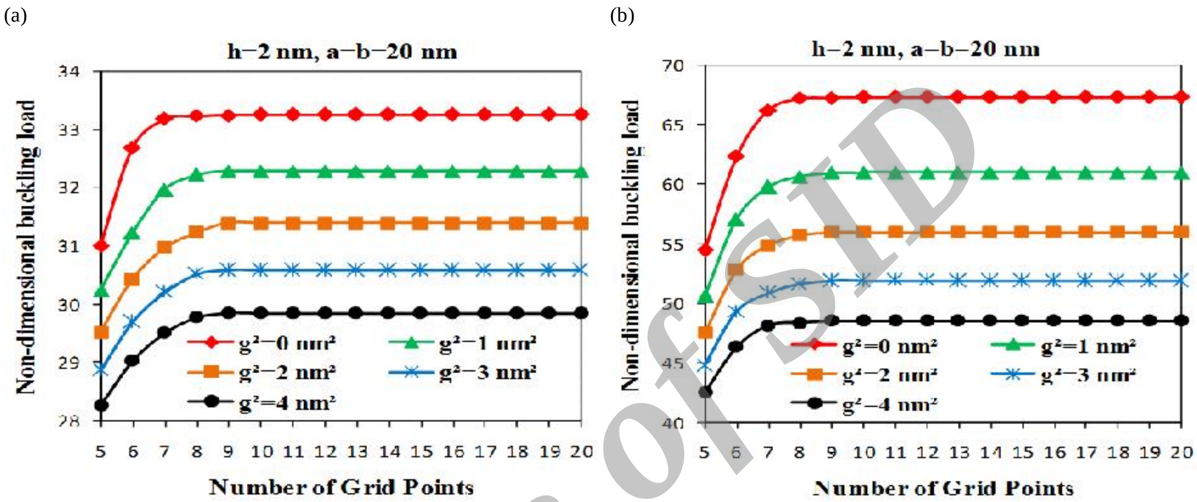

Fig. 3: Convergence study and minimum number of grid points required for obtaining accurate results for non-dimensional buckling load by finite difference method with various non-local parameter, (a) simply-support boundary conditions, (b) clamped boundary conditions,(ΔT=0° *K*)

clamped (CCCC) boundary conditions versus length and thickness nanoplates, respectively. This figure indicates that the CBLR would decrease with increasing values of non-local parameter, and this decreasing of CBLR is more pronounced for the nanoplate with the clamped boundary conditions. It is observed in Fig. 4(a) that when the nanoplate length reaches a certain value (e.g. 50 *nm*), the non-local effect disappears. Also, it can be seen in Fig. 4(b) that by increasing nanoplate thickness (h=1-2 *nm*), the CBLR would diminish heavily. Therefore, the influence of surface effect on the CBLR is more significant when the length and thickness of nanoplates would increase and decrease, respectively.

Fig. 5 shows the variation of load ratio versus non-local parameter (g^2) for different temperature changes (ΔT=0-120° *K*) and with simply-supported and clamped boundary conditions. The length and thickness of nanoplates in Fig. 5 were considered as a=40 *nm* and h=3 *nm*, respectively. The influences of surface energy and residual surface stress have not been taken into account (E^s=τ^s=0 *N/m*). Here, the temperature change is considered at a low, or at room, temperature. Therefore, the thermal expansion is α=1.9×K^{-1} [33]. According to Fig. 5, the CBLR would decrease with increasing values of non-local parameter, and this decreasing of CBLR more pronounced for the nanoplate with the clamped boundary conditions. On the other hand, it is observed that as the value of temperature change increases, the CBLR would decrease. This means that the small-scale effects increase with increasing the temperature changes. This situation is more pronounced for the nanoplate with simply-supported boundary conditions.

Figs. 6 (a and b) illustrate the variation of CBLR with non-local parameter for various surface residual stresses and for simply-supported and clamped boundary conditions, respectively. The temperature change, length and the thickness of nanoplate in all the examples were considered as ΔT=40° *K*, a=15 *nm*

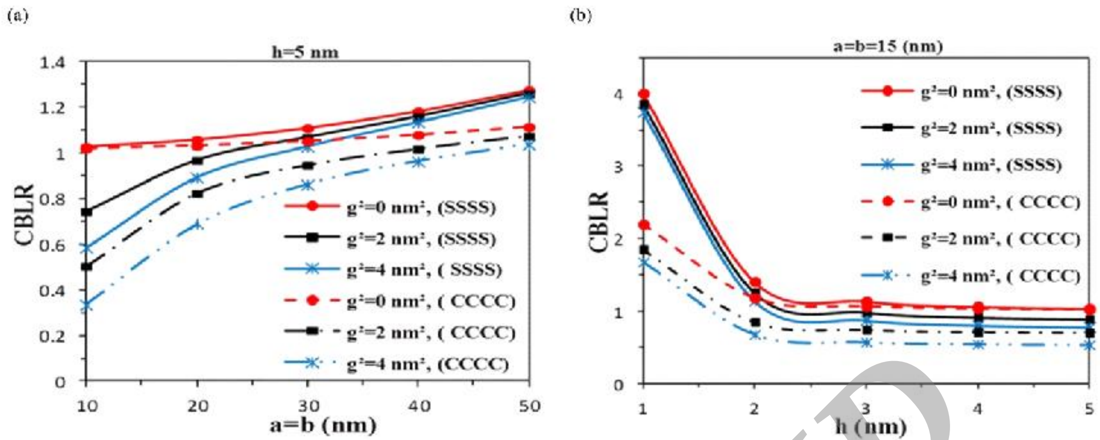

Fig. 4: Changes of the critical buckling load ratio for different non-local parameters, (a) versus length nanoplates, (b) versus thickness nanoplates.

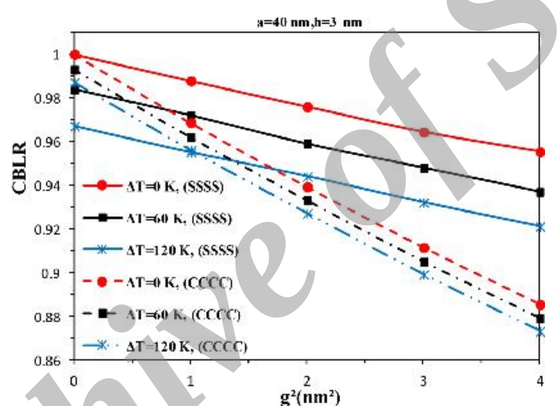

Fig. 5: Changes of the buckling load ratio with non-local parameters for different temperatures (E^s=τ^s=0 *N/m*).

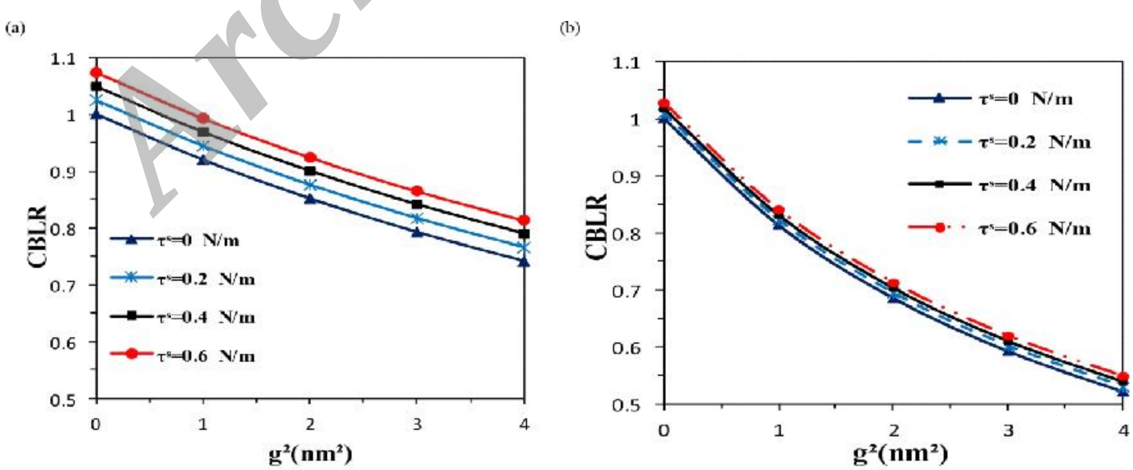

Fig. 6: Change of load ratio with non-local parameter for various values of surface residual stress, (a) simply-supported boundary conditions, (b) clamped boundary conditions (E^s=0 *N/m*)

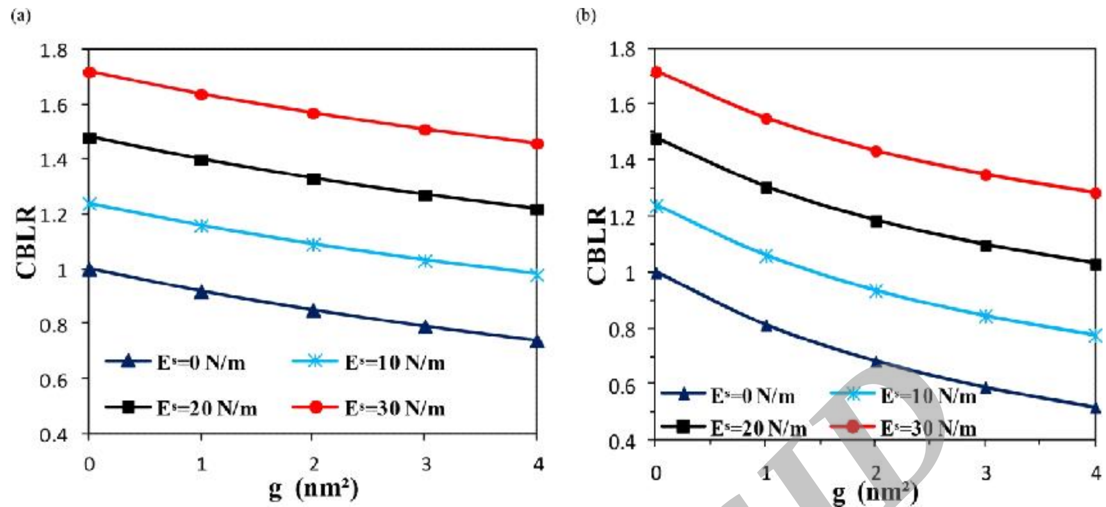

Fig. 7: Change of load ratio with non-local parameter for different values of surface elasticity modulus, (a) simply-supported boundary conditions, (b) clamped boundary conditions (τ^s=0 *N/m*).

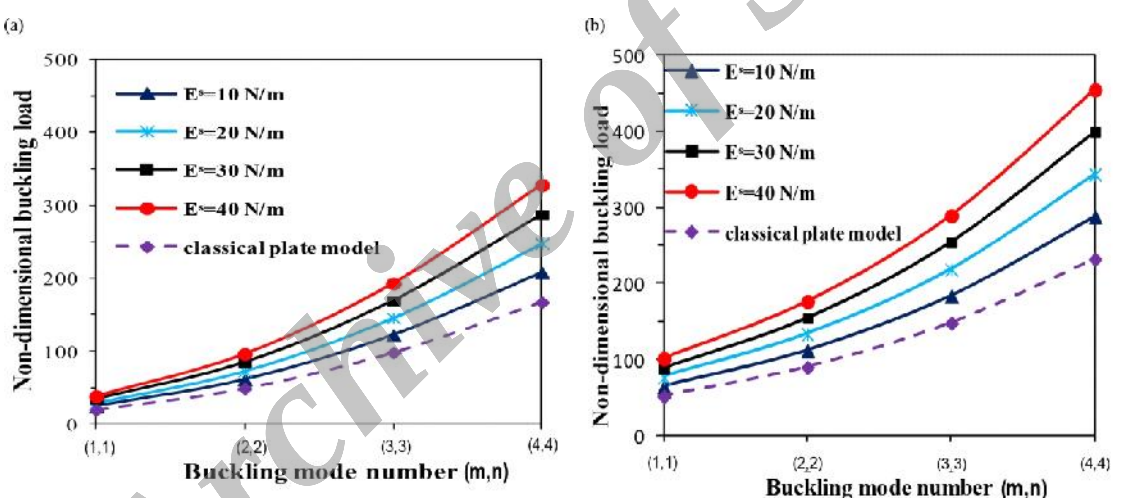

Fig. 8: Surface energy effects on the higher buckling modes of rectangular nanoplates, (a) simply-supported boundary conditions, (b) clamped boundary conditions; *m*=1:4 and *n*=1:4 are the half-wave number (buckling modes) along x and y directions, respectively; (τ^s=0.1 *N/m*)

and *h*=3 *nm*, respectively, unless noted otherwise. The influences of surface energy have not been taken into account (E^s=0 *N/m*). Again, it is clearly seen that the CBLR decreases with increasing non-local parameter. Moreover, the CBLR increases with improving surface residual stress. This observation means that the non-local effects diminish with increasing surface residual stress. In addition, by comparing Fig. 6(a) and Fig. 6(b), it can be found that the buckling load ratio in Fig. 6(a) is more sensitive to the surface residual stress.

Fig. 7 (a and b) show the variation of load ratio with non-local parameter for different surface elastic modulus and for simply-supported and clamped boundary conditions, respectively. The influences of surface residual stress have not been taken into consideration (τ^s=0 *N/m*). It is seen that when the surface elastic modulus increases, the CBLR would augment. In other words, with increasing the value of elastic modulus, the non-local effects could diminish.

To show the influence of surface energy on the higher modes of buckling nanoplates, the variation of non-dimensional buckling load ($N a^2/D$) versus mode number, *m*, for various surface elastic modulus have been shown in Fig. 8(a and b), respectively. Simply-supported and clamped boundary conditions are investigated in two figures. In Fig. 8(a and b), m=1:4 and n=1:4 are the half-wave number (buckling modes) along x and y directions, respectively. To focus on the effect of surface elastic modulus, the non-local parameter is assumed to be zero (g^2 (nm^2)). It is found that by increasing the surface elastic modulus, the non-dimensional buckling load would increase. On the other hand, the gap between the curves gradually widens with increasing buckling mode number. This means that the surface effects are more significant in higher buckling modes.

CONCLUSION

In this study, FDM was used to solve sixth-order derivatives of differential equations in buckling analysis of nanoplates due to coupled surface energy and non-local elasticity theories. The uniform temperature change was used to study thermal effect. The small scale and surface energy effects are added into the governing equations using Eringen's non-local elasticity and Gurtin-Murdoch's theories, respectively. Two different boundary conditions including simply-supported and clamped boundary conditions are investigated. The governing differential equation is introduced according to the literature, and then this equation is solved using the FDM to obtain the buckling for several combinations of boundary conditions. To verify the accuracy of the results obtained by the FDM, these results are compared with the results of the analytical approach. From the results of the present work, the following conclusions were important:

- The finite difference method could be used as a powerful method to determine the mechanical behavior of nanoplates. Moreover, this method could be used to solve higher-order derivatives of differential equations with different types of boundary condition with little computational effort.
- The surface effects on the CBLR of nanoplates increased with increasing nanoplate length and decreasing non-local parameter and nanoplate thickness.
- The non-local parameter decreased with increasing in the values of surface residual stress, surface elastic modulus and decreasing in the degree of temperature change. This means that the surface effects were more significant when the values of surface residual stress, surface elastic modulus increased and the temperature change decreased.
- The non-dimensional buckling load increased with rising in the values of surface elastic modulus and mode numbers. This means that the surface effects are more important in higher buckling modes.

In all the findings, the CBLR values were always higher for nanoplates with simply-supported boundary conditions than those with clamped boundary conditions.

NOMENCLATURE

E	Modulus of elasticity
E^s	Surface elastic modulus
¬	Poisson's ratio
τ^s	Surface residual stress
λ^s, μ^s	Surface Lame constants
$£_{ij}$	Strain components
$\pm_{ij}^{s}$	Surface stress components
$\pm_{ij}^{b}$	Bulk stress components
M_{ij}	Bending moment components
D	Flexural rigidity
x,y,z	Cartesian coordinates
u, v, w	Displacements in the x, y and z directions, respectively
a, b, h	Length, width and thickness of nanoplate, respectively
r_x, r_y	Distance between two grid points in the x and y directions, respectively

Superscripts

$( )^+$, $( )^-$	Upper and lower surfaces of nanoplate, respectively
$( )^s$	Surface of nanoplate

Subscripts

$( )_{,x}$, $( )_{,y}$	Partial derivatives with respect to x and y, respectively

REFERENCES

[1] Sakhaee-Pour A., Ahmadian M. T., Vafai, A., (2008), Applications of single-layered graphene sheets as mass sensors and atomistic dust detectors. *Solid State Commun.* 145: 168-172.

[2] Wang Z. L., Song J., (2006), Piezoelectric nanogenerators based on zinc oxide nanowire arrays. *Science.* 312: 242–246.

[3] Gurtin M. E., Murdoch A. I., (1975), A continuum theory of elastic material surfaces. *Arch. Ration. Mech. Anal.* 57: 291–323.

[4] Gurtin M. E, Murdoch A. I., (1978), Surface stress in solids. *Int. J. Solids Struct.* 14: 431–440.

[5] Assadi A., Farshi B., Alinia-Ziazi A., (2010), Size dependent dynamic analysis of nanoplates. *J. Appl. Phys.* 107: 124310.

[6] Assadi A., (2013), Size dependent forced vibration of nanoplates with consideration of surface effects. *Appl. Math. Model.* 37: 3575–3588.

[7] Assadi A., Farshi B., (2010), Vibration characteristics of circular nanoplates. *J. Appl. Phys.* 108: 074312.

[8] Assadi A., Farshi B., (2011), Size dependent stability analysis of circular ultrathin films in elastic medium with consideration of surface energies. *Physica E.* 43: 1111–1117.

[9] Ansari R., Sahmani S., (2011), Bending behavior and buckling of nanobeams including surface stress effects corresponding to different beam theories. *Int. J. Mech. Sci.* 49: 1244–1255.

[10] Challamel N., Elishakoff I., (2012), Surface stress effects may induce softening: Euler–Bernoulli and Timoshenko buckling solutions. *Physica E.* 44: 1862–1867.

[11] Karimi M., Shokrani M. H., Shahidi A. R., (2015), Size-dependent free vibration analysis of rectangular nanoplates with the consideration of surface effects using finite difference method. *J. Applied Comput. Mech.* 1: 122-133.

[12] Ansari R., Shahabodini A., Shojaei M. F., Mohammadi V., Gholami R., (2014), On the bending and buckling behaviors of Mindlin nanoplates considering surface energies. *Physica E.* 57: 126–137.

[13] Ansari R., Mohammadi V., Faghih Shojaei M., Gholami R., Sahmani S., (2014), On the forced vibration analysis of Timoshenko nanobeams based on the surface stress elasticity theory. *Compos Part B.* 60: 158–166.

[14] Mouloodi S., Khojasteh J., Salehi M., Mohebbi S., (2014), Size dependent free vibration analysis of Multicrystalline nanoplates by considering surface effects as well as interface region. *Int. J. Mech. Sci.* 85: 160–167.

[15] Mouloodi S., Mohebbi S., Khojasteh J., Salehi M., (2014), Size-dependent static characteristics of multicrystalline nanoplates by considering surface effects. *Int. J. Mech. Sci.* 79: 162–167.

[16] Wang K. F., Wang B. L., (2013), A finite element model for the bending and vibration of nanoscale plates with surface effect. Finite. *Elem. Anal. Des.* 74: 22–29.

[17] Wang K. F., Wang B. L., (2011), Combining effects of surface energy and non-local elasticity on the buckling of nanoplates. *Micro Nano Lett.* 6: 941–943.

[18] Wang K. F., Wang B. L., (2011), Vibration of nanoscale plates with surface energy via nonlocal elasticity. *Physica E.* 44: 448–453.

[19] Farajpour A., Dehghany M., Shahidi A. R., (2013), Surface and nonlocal effects on the axisymmetric buckling of circular graphene sheets in thermal environment. *Compos. Part B.* 50: 333–343.

[20] Asemi S. R., Farajpour A., (2014), Decoupling the nonlocal elasticity equations for thermo-mechanical vibration of circular graphene sheets including surface effects. *Physica E.* 60: 80–90.

[21] Mahmoud F. F., Eltaher M. A., Alshorbagy A. E., Meletis E. I., (2012), Static analysis of nanobeams including surface effects by nonlocal finite element. *J. Mech. Sci. Tech.* 26: 3555–3563.

[22] Eltaher M. A., Mahmoud F. F., Assie A. E., Meletis E. I., (2013), Coupling effects of nonlocal and surface energy on vibration analysis of nanobeams. *Appl. Math. Comput.* 224: 760–774.

[23] Karimi M., Haddad H. A., Shahidi A. R., (2015), Combining surface effects and non-local two variable refined plate theories on the shear/biaxial buckling and vibration of silver nanoplates. *Micro and Nano Lett.* 10: 276-281.

[24] Shokrani M. H., Karimi M., Tehrani M. S., Mirdamadi H. R., (2015), Buckling analysis of double-orthotropic nanoplates embedded in elastic media based on non-local two-variable refined plate theory using the GDQ method. *J. Braz. Soc. Mech. Sci. Eng.* DOI: 10.1007/s40430-015-0370-0

[25] Sheikholeslami M., Rashidi M. M., (2015), Effect of space dependent magnetic field on free convection of Fe_3O_4-water nanofluid. *J. Taiwan Inst. Chem. Eng.* DOI: 10.1016/j.jtice.2015.03.035.

[26] Sheikholeslami M., ganji D. D., (2014), Nanofluid flow and heat transfer between parallel plates considering Brownian motion using DTM. *Comput. Methods Appl. Mech. Eng.* 283: 651–663.

[27] Sheikholeslami M., Bandpy M. G., Ashorynejad H. R., (2015), Lattice Boltzmann Method for simulation of magnetic field effect on hydrothermal behavior of nanofluid in a cubic cavity. *Physica A.* DOI: 10.1016/j.physa.2015.03.009

[28] Sheikholeslami M., Bandpy M. G., ganji D. D., (2012), Magnetic field effects on natural convection around a horizontal circular cylinder inside a square enclosure filled with nanofluid. *Int. Commun. Heat Mass.* 39: 978–986

[29] Soleimani S., Sheikholeslami M., ganji D. D., Bandpy M. G., (2012), Natural convection heat transfer in a nanofluid filled semi-annulus enclosure. *Int. Commun. Heat Mass.* 39: 565–574.

[30] Eringen A. C., Edelen D. G. B., (1972), On nonlocal elasticity. *Int. J. Mech. Sci.* 10: 233–248.

[31] Karamooz Ravari M. R., Talebi S., Shahidi A. R., (2014), Analysis of the buckling of rectangular nanoplates by use of finite-difference method. *Meccanica.* 49: 1443–1455.
[32] Karamooz Ravari M. R., Shahidi A. R., (2013), Axisymmetric buckling of the circular annular nanoplates using finite difference method. *Meccanica.* 48: 135–144.
[33] Greer J. R, Street R. A., (2007), Mechanical characterization of solution-derived nanoparticle silver ink thin films. *J. Appl. Phys.* 101: 103529.

How to cite this article: (Vancouver style)
Karimi M, Shahidi A. R., (2015), Finite difference method for sixth-order derivatives of differential equations in buckling of nanoplates due to coupled surface energy and non-local elasticity theories. *Int. J. Nano Dimens.* 6(5): 525-537.
DOI: 10.7508/ijnd.2015.05.010
URL: http://ijnd.ir/article_17146_1117.html